Growth Properties of Colonic Tumor Cells Are a Function of the Intrinsic Mitochondrial Membrane Potential

Barbara G. Heerdt, Michele A. Houston, and Leonard H. Augenlicht

Department of Oncology, Albert Einstein Cancer Center, Montefiore Medical Center, Bronx, New York

Abstract

Development of malignant transformation in the colonic mucosa includes disruption in the equilibrium between proliferation and apoptosis, decreased expression and deletions of the mitochondrial genome, alterations in mitochondrial enzymatic activity, and elevations in the mitochondrial membrane potential ($\Delta\psi m$). Focusing on the role of the $\Delta\psi m$ in tumor development and progression, we generated novel isogenic colonic carcinoma cell lines that exhibit highly significant, stable differences in their intrinsic $\Delta\psi m$. Using these cell lines, we have recently shown that the intrinsic $\Delta\psi m$ has a significant influence on steady state mitochondrial activity and the extent to which cells enter butyrate-mediated growth arrest and apoptotic cascades. Here, we report that the $\Delta\psi m$ is also profoundly linked to important tumorigenic properties of the cells. Compared with cells with lower $\Delta\psi m$, cells with elevated intrinsic $\Delta\psi m$ have an enhanced capacity to (*a*) respond to hypoxia by avoiding apoptosis and initiating angiogenesis, (*b*) escape anoikis and grow under anchorage-independent conditions, and (*c*) invade the basement membrane. Combined with our previous work, these data implicate the intrinsic $\Delta\psi m$ of colonic carcinoma cells in determining the probability of tumor expansion and progression. (Cancer Res 2006; 66(3): 1591-6)

Introduction

The colonic mucosa has one of the highest proliferative rates of any adult tissue, with stem cells near the base of the crypt producing $\sim 10^7$ new cells every hour (1, 2). As a consequence of this rapid proliferation, over a life span of six to seven decades, $>10^{12}$ cell divisions will have taken place in the colonic mucosa. For >90% of patients with colon cancer, the initiation of tumorigenesis is linked to only one of these cell divisions. Therefore, it is likely that subtle shifts in biochemical pathways and/or cell composition have the potential of dramatically affecting the probability of tumor formation.

Our previous work has shown that regardless of the etiology, early steps in the malignant transformation of colonic epithelial cells include depressed expression of the mitochondrial genome (3, 4). Other studies have shown that the subsequent development and progression of colonic tumors are linked to mutations and deletions in the mitochondrial genome (5, 6), alterations in mitochondrial enzymatic activity (7, 8) and elevations in the mitochondrial membrane potential ($\Delta\psi m$; refs. 9–13).

Focusing on the $\Delta\psi m$, we have shown the necessity for an intact $\Delta\psi m$ in the initiation of both cell cycle arrest and apoptosis of colonic carcinoma cells induced by the short-chain fatty acid butyrate (NaB), a product of fiber fermentation that is found at high concentrations in the colonic lumen and used by colonic epithelial cells as their principle source of energy (14, 15). More recently, we developed novel isogenic colonic carcinoma cell lines that exhibit subtle, stable differences in their intrinsic $\Delta\psi m$, and showed that these differences in $\Delta\psi m$ significantly affect steady state mitochondrial gene expression and the extent to which cells enter short-chain fatty acid butyrate–mediated growth arrest and apoptotic cascades (15).

We have dissected the functional effect of differences in the $\Delta\psi m$, asking whether they were associated with cellular properties that characterize the enhanced probability of colonic tumor expansion and progression. We report here that the modest, but significant, stable differences in the intrinsic $\Delta\psi m$ exhibited by the isogenic cell lines are linked to the cell's response to hypoxia, the ability to survive and grow under anchorage-independent conditions, and the capacity to invade the basement. These data show that differences in the intrinsic $\Delta\psi m$ of colonic carcinoma cells are likely tied to the subtle shifts in biochemical pathways and/or cell phenotype that play fundamental roles in determining the probability of colonic tumor progression (15, 16).

Materials and Methods

Generation of isogenic cell lines that exhibit significant stable differences in intrinsic $\Delta\psi m$. We have previously described the establishment of the isogenic cell lines used in this study (15). Briefly, confluent cultures of SW620 human colonic carcinoma cells (17), obtained from American Type Culture Collection (Manassas, VA) were treated for 24 hours with rotenone, antimycin A, or oligomycin B, each at 12.5 μmol/L; azide at 500 μmol/L; or nigericin at 5 μmol/L (all agents obtained from Sigma-Aldrich, St. Louis, MO) as we have previously described (14, 18, 19). Shed cells were recovered from the conditioned medium, washed, and plated in the absence of the agent. Individual clones that arose from the plated cells were selected and expanded. The resulting isogenic cell lines were maintained in MEM plus 10% fetal bovine serum. The lines are referred to as R, AA, Az, OB, or N, abbreviations of the agent to which parental cells were exposed. It is critical to note that the isogenic cell lines were maintained, and that all of the experiments using the cell lines were done in the absence of the mitochondria-targeted agents.

Determination of $\Delta\psi m$. Cells were stained with the $\Delta\psi m$-dependent fluorescent dye JC-1 (5,5′6,6′-tetrachloro-1,1′,3,3′ tetraethylbenzimidazol carbocyanineiodide; Molecular Probes, Eugene, OR) and analyzed by flow cytometry in FL-2 as we have previously described (14, 15, 19, 20).

Cell cycle variables and quantitation of apoptosis. Cells were stained with propidium iodide and analyzed by flow cytometry, as we have previously described (14, 18, 19).

Note: Supplementary data for this article are available at Cancer Research Online (http://cancerres.aacrjournals.org/).

Requests for reprints: Barbara G. Heerdt, Department of Oncology, Albert Einstein Cancer Center, Montefiore Medical Center, 111 East 210th Street, Bronx, NY 10467. Phone: 718-920-2750; Fax: 718-882-4464; E-mail: heerdt@aecom.yu.edu.

doi:10.1158/0008-5472.CAN-05-2717

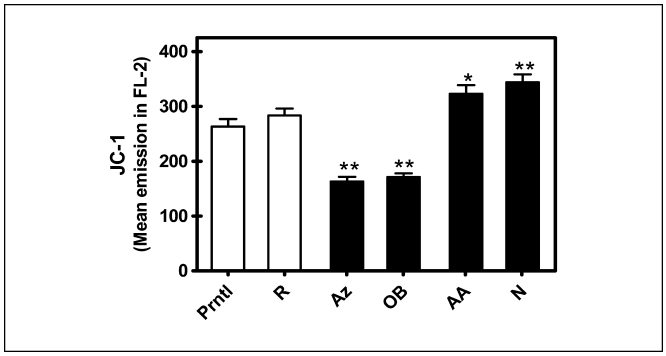

Figure 1. Differences in the intrinsic $\Delta\psi m$ among isogenic cell lines. Cells were stained with JC-1 and evaluated in FL-2 by flow cytometry. *Columns*, mean of at least three determinations; *bars*, ± SE. Significant differences in the intrinsic $\Delta\psi m$ of the isogenic cell lines compared with that of parental cells, as determined by Newman-Keuls multiple comparison tests, are indicated: *, $P < 0.01$; **, $P < 0.001$.

Quantiation of active caspase-3 and caspase-9. Active caspase-3 was quantified using phycoerythrin-conjugated anti-active caspsase-3 (PharMingen, San Diego, CA) followed by flow cytometry, as we have previously described (19). Active caspase-9 was quantified by staining cells with Red-LEHD-FMK (Oncogene Research Products, San Diego, CA), which binds irreversibly to active caspase-9 in living cells, and analyzing fluorescence of the dye by flow cytometry in the FL-2 channel.

Response to hypoxia. Cells in replicate 96-well plates were grown to ~80% confluence for 6 days before $CoCl_2$ was added to a final concentration of 100 μmol/L. Twenty-four hours later, one of the plates was used to determine the number of viable cells by the spectrophotometric quantitation of reduction of the tetrazolium salt methylthiazoletetrazolium (Sigma-Aldrich) to formazan (21), and a standard curve generated by serial dilution of parental SW620 cells. Cells collected from replicate plates were stained with JC-1 for determination of $\Delta\psi m$, or lysed for quantitation of $p21^{WAF1/Cip1}$ or Bcl2 by ELISA (Oncogene Research Products, La Jolla, CA) according to the manufacturer's protocol. Conditioned medium was collected from replicate plates and used for quantitation of vascular endothelial growth factor (VEGF) by ELISA (R&D Systems, Inc., Minneapolis, MN) according to the manufacturer's protocol.

Cell invasion. Cell invasion was determined employing a system that uses a matrix of reconstituted basement membrane protein, derived form the Engelbreth Holm-Swam mouse tumor, overlaying an 8-μm pore size polycarbonate membrane (Chemicon, Temecula, CA). SW620 and isogenic cell lines were seeded on top of the basement membrane layer, as described by the manufacturer, and incubated at 37°C for 24 hours. The cells that migrated through, and adhered to the bottom of the polycarbonate membrane, were stained and quantified by absorbance.

Evaluation of growth properties. To evaluate the effect of differences in $\Delta\psi m$ on anchorage-independent growth, parental SW620 and isogenic cells were seeded at 1.5×10^4 cells/well into 96-well Ultralow adhesion plates (ULA; Costar, Corning, Inc., Corning, NY), plates that we coated with polyHEMA as described (22), or standard tissue culture treated plates (Falcon, Becton Dickinson Labware, Franklin Lakes, NJ). Viable cell number was determined at 2-day intervals for 8 days by the spectrophotometric quantitation of methylthiazoletetrazolium reduction to formazan (21) based on a standard curve generated by parental cells. Growth was confirmed by determination of total cellular protein/well using Bio-Rad protein reagent (Bio-Rad Laboratories, Hercules, CA) according to the manufacturer's protocol.

Statistical analyses. Data from at least three independent determinations were compared by Newman-Keuls and Bonferroni's multiple comparison tests. Mean data were also evaluated as a function of intrinsic $\Delta\psi m$, determined by JC-1 staining, using linear regression analyses.

Results

Isogenic cell lines with differences in intrinsic $\Delta\psi m$ as a system to study the effect of the $\Delta\psi m$ on colonic carcinoma cell function. These studies used five isogenic cell lines, referred to as R, Az, OB, AA, and N, which were generated as previously described (15). Cells stained with the $\Delta\psi m$-sensitive dye JC-1 (23–25) and analyzed by flow cytometry in fluorescence detection channel 2 (FL-2), has established that compared with the parental SW620 cells, the intrinsic $\Delta\psi m$ of two of these lines, the Az and the OB lines, is significantly decreased; the $\Delta\psi m$ of two lines, the AA and the N lines, is significantly elevated; and the $\Delta\psi m$ of the R line is comparable to that of parental cells (Fig. 1). Furthermore, whereas the intrinsic $\Delta\psi m$ of the AA and N lines are similar to one another, as are the $\Delta\psi m$ of the Az and OB lines, the differences in the intrinsic $\Delta\psi m$ between the isogenic lines with high (AA and N) and low (Az and OB) $\Delta\psi m$ are ~2-fold, and highly significant (Table 1).

Whereas the differences in $\Delta\psi m$ among the cell lines are highly significant, they are modest. It is important to appreciate that greater differences in the intrinsic $\Delta\psi m$ would likely promote the generation and accumulation of reactive oxygen species, and disrupt electron transport/oxidative phosphorylation as well as the mitochondrial import and subsequent processing of nuclear encoded peptides (26–29). The consequence of such perturbations in essential mitochondrial functions would be loss of viability. Therefore, these isogenic cell lines provide an excellent system with which to dissect the relationship between differences in the intrinsic $\Delta\psi m$ that are compatible with cell viability and colonic carcinoma cell function and phenotype.

Differences in the intrinsic $\Delta\psi m$ are linked to the cellular response to hypoxia and nonadherent conditions. Expansion and progression of solid tumors inevitably results in areas within the tumor in which the demand for oxygen by growing neoplastic cells exceeds the amount that can be obtained by diffusion from existing blood vessels. As a result, regions of the tumor become hypoxic. Although cells that are unable to tolerate an oxygen-poor microenvironment become necrotic or apoptotic, other cells survive by decreasing their growth rate, and/or activating pathways that block apoptosis and initiate the formation of new blood vessels. Thus, the cellular response to hypoxia could act as a selective pressure, favoring the expansion of cells that can adapt to an oxygen-poor environment.

Similar to hypoxia, $CoCl_2$ inhibits the degradation of the α subunit of the hypoxia-inducible factor 1 (HIF-1), resulting in

Table 1. Comparison of $\Delta\psi m$ of isogenic cell lines

Cell lines compared	Fold difference	Newman-Keuls multiple comparison test (*P* values)
R vs. AA	1.14	<0.050
R vs. Az	0.58	<0.001
R vs. OB	0.60	<0.001
R vs. N	1.21	<0.010
AA vs. Az	0.51	<0.001
AA vs. OB	0.53	<0.001
AA vs. N	1.06	>0.050
Az vs. OB	1.05	>0.050
Az vs. N	2.11	<0.001
OB vs. N	2.01	<0.001

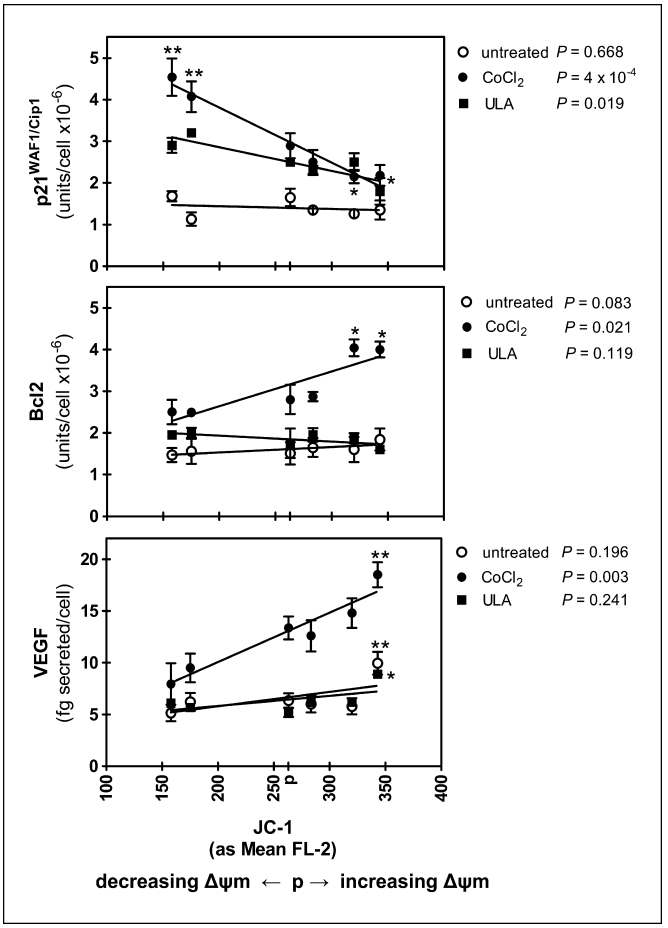

Figure 2. Differences in the intrinsic Δψm are linked to the cellular response to hypoxia and the nonadherent conditions. Levels of cellular $p21^{WAF1/Cip1}$ and Bcl2, and secreted VEGF, were quantified in cell lysates or conditioned medium, respectively, from untreated cells (○), cells exposed to $CoCl_2$-mediated hypoxia for 24 hours (●) or cells grown under anchorage-independent conditions in ULA plates for 4 days (■). Mean ± SEM of at least three determinations are plotted as a function of the intrinsic Δψm of each cell line, as determined by mean emission of JC-1 in FL-2. The emission of JC-1 by parental cells is indicated by the "p" on the horizontal axis. *P* values from linear regression analyses (*right*). Significant differences are indicated in the levels of $p21^{WAF/Cip1}$, Bcl2, or VEGF in isogenic cell lines compared with similarly treated parental cells, as determined by Bonferroni's multiple comparison tests: *, $P < 0.01$; **, $P < 0.001$.

HIF-1α accumulation (30). HIF-1α controls the cellular responses to hypoxia, activating the transcription of a number of genes, including those involved in modulation of proliferation, apoptosis, and angiogenesis (31–38). To address the question of whether differences in the intrinsic Δψm were linked to the ability of colonic carcinoma cells to adapt and respond to hypoxic conditions, the isogenic and parental cell lines were exposed to $CoCl_2$-simulated hypoxia for 24 hours. Levels of cellular $p21^{WAF/Cip1}$ and Bcl2, as well as secreted VEGF, were then quantified, expressed per viable cell, and plotted as a function of the intrinsic Δψm of the cell line (i.e., linear regression; Fig. 2).

Consistent with it being a HIF-1α–responsive gene (39), $p21^{WAF/Cip1}$ was induced in each of the cell lines following exposure to $CoCl_2$ (Fig. 2; *closed circles*). However, compared with parental cells, the levels of induction were higher in cells with decreased intrinsic Δψm, lower in cells with elevated Δψm, and inversely linked to the intrinsic Δψm ($P = 4 \times 10^{-4}$ from linear regression).

Unlike $p21^{WAF/Cip1}$, the antiapoptotic protein Bcl2 is not transcriptionally regulated by HIF-1α (40). Nonetheless, compared with untreated cells, Bcl2 protein levels were increased in each of the cell lines following exposure to $CoCl_2$-mediated hypoxia. Moreover, whereas the levels of Bcl2 in the cell lines with decreased Δψm were similar to that induced in parental cells, the levels in cells with increased intrinsic Δψm were significantly higher, and there was a significant correlation between the intrinsic Δψm and Bcl2 levels ($P = 0.021$).

As expected, levels of VEGF, a major HIF-1α target gene which stimulates the migration of endothelial cells into tumors to form new microvessels, increased in each of the cell lines following exposure to $CoCl_2$-mediated hypoxia. However, compared with parental cells, the levels of induction were significantly higher in the cells with elevated Δψm, lower in cells with decreased Δψm and there was a significant relationship between the intrinsic Δψm and VEGF production ($P = 0.003$). Importantly, the level of VEGF secreted from untreated cells with the highest intrinsic Δψm, the N cell line, was significantly higher than that of parental cells ($P < 0.001$). We have recently reported that in subclones derived from untreated SW620 cells, similar significant elevations in steady state VEGF production are detected in cell lines with elevated intrinsic Δψm (41).

Because tumor progression could also lead to the selection of cells that have the ability to survive and grow under anchorage-independent conditions, cells were seeded into standard tissue culture wells, a substratum that promotes cellular adhesion, or

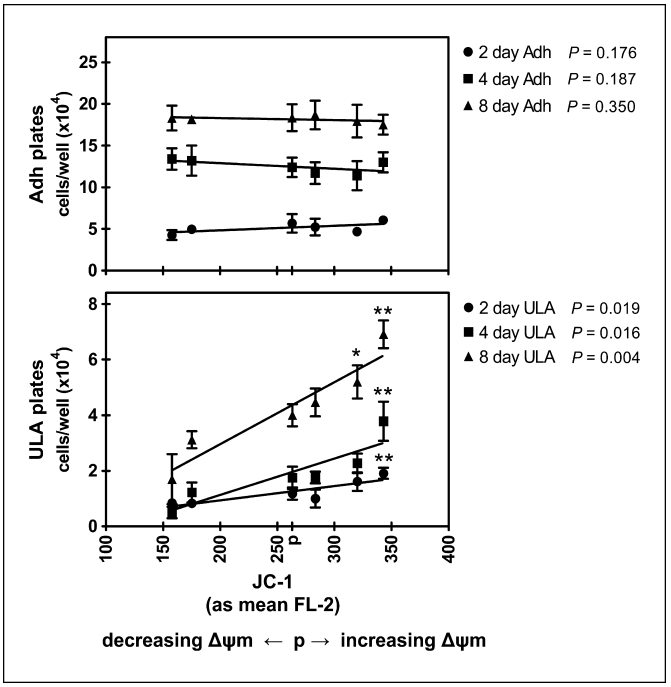

Figure 3. Differences in the intrinsic Δψm are linked to the ability of cells to grow under anchorage-independent conditions. Cells were seeded in standard tissue culture–treated plates, which promote adhesion (Adh), or in ULA plates, which block attachment of cells to a substratum. The number of viable cells was determined at 2 (●), 4 (■), and 8 (▲) days following seeding. Mean ± SEM of at least three determinations are plotted as a function of intrinsic Δψm of each cell line, as determined by mean emission of JC-1 in FL-2. Emission of JC-1 by parental cells is indicated as "p" on the horizontal axis. *P* values from linear regression analyses (*right*). Statistical analysis of viable isogenic cells, compared with parental cells, by Bonferroni's multiple comparison tests: *, $P < 0.01$; **, $P < 0.001$.

into ULA wells, which block adherence. The number of viable cells was determined 2, 4, and 8 days after seeding and analyzed as a function of the intrinsic $\Delta\psi m$ of the cell line (Fig. 3).

When grown under adherent conditions, the differences in the $\Delta\psi m$ had no effect on cell number or growth rates at either 2, 4, or 8 days. In marked contrast, when grown under anchorage-independent conditions, there was a significant association between the intrinsic $\Delta\psi m$ and cell number and growth rates. Compared with parental cells, there was less extensive and slower growth of cells with decreased intrinsic $\Delta\psi m$, but more extensive and faster growth in cells with increased $\Delta\psi m$. Moreover, the relationship between the intrinsic $\Delta\psi m$ and the ability of cells to undergo anchorage-independent growth increased over time (P values from linear regression analyses range from 0.019 at 2 days to 0.004 at 8 days). The relationship between the $\Delta\psi m$ and the ability of cells to grow under anchorage-independent conditions was confirmed using a different source of ULA plates, those that we coated with polyHEMA, and total cellular protein as an index of cell number (Supplemental Figs. S1 and S2, respectively).

To further investigate variations in the ability of cells with different intrinsic $\Delta\psi m$ to survive and grow under anchorage-independent conditions, cells were seeded into ULA plates and allowed to grow for 4 days. Levels of $p21^{WAF/Cip1}$, Bcl2, and secreted VEGF were then quantified, expressed per viable cell, and plotted as a function of the intrinsic $\Delta\psi m$ of the cell line (Fig. 2; closed squares).

With the exception of the cell line with the highest intrinsic $\Delta\psi m$, $p21^{WAF/Cip1}$ levels in cells grown under nonadherent conditions were higher than those in cells grown under adherent conditions, but not as high as in $CoCl_2$-treated cells, and inversely linked to the intrinsic $\Delta\psi m$ ($P = 0.019$). In contrast, levels of Bcl2 and VEGF in viable nonadherent cells were comparable with those of adherent cells, and were not associated with differences in the intrinsic $\Delta\psi m$ ($P = 0.119$ and $P = 0.241$, respectively). However, it is noteworthy that, as seen in the adherent cells and consistent with our recent work (41), the level of VEGF secreted from anchorage-independent cells with the highest $\Delta\psi m$ was significantly higher than that of nonadherent parental cells ($P < 0.01$).

We next asked whether the $\Delta\psi m$-associated modulations in $p21^{WAF/Cip1}$ levels in cells subjected to $CoCl_2$-mediated hypoxia or nonadherent conditions were linked to growth arrest. For these studies, we focused on the cell lines with the lowest and highest intrinsic $\Delta\psi m$ (the Az and N lines, respectively; Fig. 1; Table 1).

As shown in Fig. 4*A*, compared to cells with higher $\Delta\psi m$, fewer cells with low $\Delta\psi m$ levels were in G_0-G_1, but more cells were in G_2-M, after 24-hour $CoCl_2$ treatment. In contrast, 4 days after seeding into ULA plates, more cells with low $\Delta\psi m$ levels were in G_0/G_1, but fewer in G_2-M, than cells with higher $\Delta\psi m$. $p21^{WAF/Cip1}$ could bind to G_1 cyclin-CDK complexes inducing arrest of cells in G_0-G_1, and interact with proliferating cell nuclear antigen resulting in G_2-M arrest, depending on the relative abundance of $p21^{WAF/Cip1}$, CDKs and proliferating cell nuclear antigen (42). Therefore, although the mechanism by which $p21^{WAF/Cip1}$ induces inhibition of cell cycle progression in $CoCl_2$-mediated hypoxia or anchorage-independence may differ, our data show that the magnitude of growth arrest in cells with low $\Delta\psi m$ is significantly greater than that in cells with higher intrinsic $\Delta\psi m$, consistent with higher levels of $p21^{WAF/Cip1}$ protein in these cells.

There are two main pathways to cell death by apoptosis; one triggered by death receptors on the plasma membrane, the other activated by diverse intracellular stresses. In the first pathway,

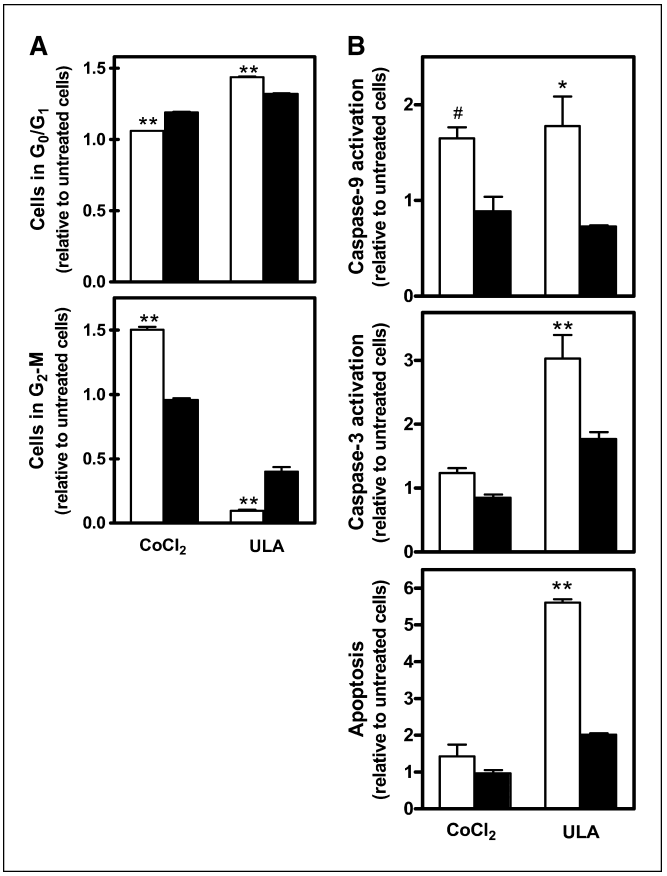

Figure 4. Differences in the intrinsic $\Delta\psi m$ are linked differences in cell cycle arrest and apoptosis induced by $CoCl_2$-mediated hypoxia and anchorage independence. The isogenic cell lines with the lowest (*open columns*, $\downarrow\Delta\psi$) and highest (*closed columns*, $\uparrow\Delta\psi$) intrinsic $\Delta\psi m$ (the Az and N lines, respectively) were exposed to $CoCl_2$-mediated hypoxia for 24 hours, or anchorage-independent growth on ULA plates for 4 days. Cell cycle variables (*A*) and activation of caspase-9 and caspase-3 (*B*), and apoptosis were quantified and expressed relative to untreated, adherent cells. *Columns*, mean of at least three determinations; *bars*, $\pm$ SE. Significant differences between the cell lines, as determined by Bonferroni's multiple comparison tests, are indicated: #, $P < 0.05$; *, $P < 0.01$; **, $P < 0.001$.

ligation of cell surface receptors typically initiates the cleavage and activation of procaspases, such as procaspase-8, which can directly activate other caspase members, including caspase-3, ultimately producing apoptosis. In the second pathway, cytochrome *c*, released from the inner mitochondrial membrane, forms a complex with procaspase-9 and Apaf1, the "apoptosome," which mediates the cleavage and activation of caspase-9. Active caspase-9 then processes other caspase members, including caspase-3, to initiate a caspase cascade that leads to apoptosis.

Because Bcl2 and other antiapoptotic family members could prevent cytochrome *c* release and, consequently, caspase-9 activation (reviewed in ref. 43), we investigated how $\Delta\psi m$-associated modulations in Bcl2 protein levels were linked to caspase activation and apoptosis. For these studies, we again focused on the cell lines with the lowest and highest intrinsic $\Delta\psi m$ and quantified caspase-9 and caspase-3 activation, and apoptosis following exposure to 24-hour $CoCl_2$-mediated hypoxia or 4-day anchorage-independent growth.

As shown in Fig. 4*B*, consistent with increased Bcl2, activation of caspase-9 and caspase-3, and apoptosis were not detected in cells with high intrinsic $\Delta\psi m$ levels following treatment with $CoCl_2$.

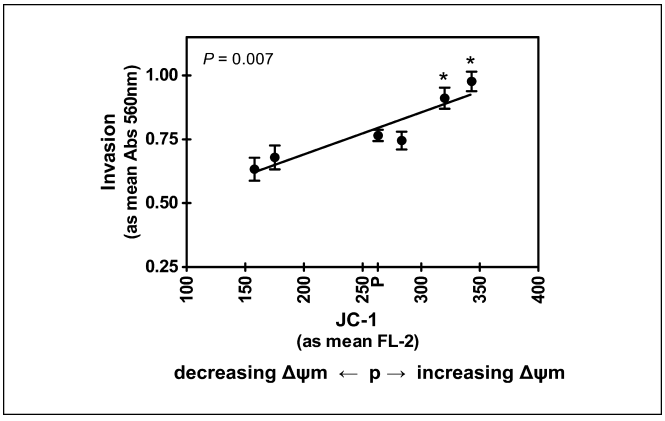

Figure 5. Differences in the intrinsic Δψm are linked to the ability of cells to cross the basement membrane. Cells were seeded on top of a matrix of reconstituted basement membrane protein. Cells that migrated through, and attached to the bottom of a supporting polycarbonate membrane, were stained and quantified by absorbance at 560 nm. Mean ± SEM of at least three determinations are plotted as a function of intrinsic Δψm of each cell line as determined by mean emission of JC-1 in FL-2. JC-1 emission by parental cells is indicated by "p" on the horizontal axis. $P = 0.007$ from linear regression analysis. Significant differences in invasiveness of isogenic cell lines, compared with that of parental cells, as determined by Bonferroni's multiple comparison tests: *, $P < 0.01$.

Caspase-9 activation was also not detected in cells with high Δψm following nonadherent growth, but caspase-3 activation and apoptosis were slightly induced, but importantly, at significantly lower levels than in cells with low intrinsic Δψm, in accord with the more robust anchorage-independent growth and survival of cells with high Δψm than those with low Δψm. This caspase-3 activation and apoptosis in the absence of activation of caspase-9 suggests that, in cells with increased Δψm, anchorage-independence may lead to low level activation of a receptor-mediated apoptotic pathway.

In cells with low Δψm, the levels of caspase-9 activation were similar following $CoCl_2$ exposure or nonadherent growth, and higher than those in cells with elevated Δψm. However, caspase-3 activation and apoptosis were significantly higher in cells seeded in ULA plates, suggesting that $CoCl_2$-mediated hypoxia might interrupt the caspase cascade in colonic carcinoma cells with low intrinsic Δψm, possibly due to increased expression of an inhibitor of apoptosis (44).[1]

The intrinsic Δψm affects the ability of cells to invade the basement membrane. Finally, tumor expansion and progression could also result in the selection of cells with the ability to invade. Successful invasion requires cells to sever interactions with surrounding cells, cross the basement membrane, and migrate through the extracellular matrix—all the while escaping anoikis (31). Because we found that cells with increased intrinsic Δψm had an increased capacity to survive under anchorage-independent conditions, and the Δψm of migrating cells (26, 45) and cells at the leading edge of a colony outgrowth in culture (12, 46) is elevated, we reasoned that differences in the intrinsic Δψm were likely also linked to the ability of cells to cross the basement membrane.

Cells were seeded onto a thin layer of extracellular matrix protein that covered a polycarbonate membrane, and 24 hours later, the cells that had migrated through the extracellular matrix layer and attached to the bottom of the polycarbonate membrane, were stained and quantified by absorbance. These absorbance data were then plotted as a function of the intrinsic Δψm of the cell line, determined by mean JC-1 emission in FL-2. As shown in Fig. 5, cells with elevated Δψm were significantly more invasive than those with lower Δψm, and the intrinsic Δψm was associated with invasion ($P = 0.007$).

Discussion

In summary, using novel isogenic colonic carcinoma cell lines that have modest, but highly significant and stable differences in Δψm, we had previously shown the influence of the intrinsic Δψm on steady state mitochondrial activity and the extent to which cells enter butyrate-mediated growth arrest and apoptotic cascades (15). Here, we showed the profound relationship between differences in the Δψm and important tumorigenic properties. Cells with higher intrinsic Δψm have an enhanced capacity to (*a*) respond to hypoxia by avoiding apoptosis and initiating angiogenesis, (*b*) escape anoikis and grow under anchorage-independent conditions, and (*c*) invade the basement membrane. Therefore, these data establish that differences in the intrinsic Δψm of colonic carcinoma cells are likely linked to shifts in biochemical pathways and/or cell composition that play fundamental roles in determining the probability of colonic tumor progression (15, 16).

Although the mechanisms involved in producing and maintaining the differences in Δψm exhibited by these isogenic cell lines are unclear, they may reflect modulations in the composition of mitochondrial membranes. The Δψm, apoptosis and metastatic potential are each affected by alterations in mitochondrial membrane phospholipids (47–51), and we have recently found a significant correlation between the expression levels of the outer mitochondrial membrane protein VDAC and the intrinsic Δψm.[1] Thus, it is likely that variations in Δψm are associated with alterations in molecular and/or biochemical processes, regulated by the nuclear genome and/or environmental factors, that affect the generation, regulation, and maintenance of mitochondrial membranes (52, 53). Defining these processes, and dissecting their effect on colonic tumor cell growth properties, are important areas for future investigation.

Acknowledgments

Received 8/1/2005; revised 11/29/2005; accepted 12/5/2005.

Grant support: Supported in part by CA93697 and P30-13330 from the National Cancer Institute.

The costs of publication of this article were defrayed in part by the payment of page charges. This article must therefore be hereby marked *advertisement* in accordance with 18 U.S.C. Section 1734 solely to indicate this fact.

[1] B.G. Heerdt and M.A. Houston, unpublished data.

References

1. Potten CS, Schofield R, Lajtha LG. A comparison of cell 0nt in bone marrow, testis and three regions of surface epithelium. Biochim Biophys Acta 1979;560:281–99.
2. Johnson LR. Regulation of gastrointestinal mucosal growth. Physiol Rev 1988;68:456–502.
3. Augenlicht LH, Wahrman MZ, Halsey H, Anderson L, Taylor J, Lipkin M. Expression of cloned sequences in biopsies of human colonic tissue and in colonic carcinoma cells induced to differentiate *in vitro*. Cancer Res 1987;47:6017–21.
4. Heerdt BG, Augenlicht LH. Changes in the number of mitochondrial genomes during human development. Exp Cell Res 1990;186:54–9.

5. Shih C, Padhy LC, Murray M, Weinberg RA. Transforming genes of carcinomas and neuroblastomas introduced into mouse fibroblasts. Nature 1981;290: 261–4.
6. Polyak K, Xia Y, Zweier JL, Kinzler KW, Vogelstein B. A model for p53-induced apoptosis. Nature 1997;389: 300–5.
7. Modica-Napolitano JS, Steele GD, Chen LB. Aberrant mitochondria in two human colon carcinoma cell lines. Cancer Res 1989;49:3369–73.
8. Sun AS, Sepkowitz K, Beller SA. A study of some mitochondrial and peroxisomal enzymes in human colonic adenocarcinoma. Lab Invest 1981;44:13–7.
9. Summerhayes IC, Lampidis TJ, Bernal SD, et al. Unusual retention of rhodamine 123 by mitochondria in muscle and carcinoma cells. Proc Natl Acad Sci U S A 1982;79:5292–6.
10. Chen LB. Mitochondrial membrane potential in living cells. Annu Rev Cell Biol 1988;4:155–81.
11. Wong JR, Chen LB. Recent advances in the study of mitochondria in living cells. Advances in cell biology: JAI Press, Inc.; 1988. p. 263–90.
12. Chen LB, Rivers EN. Mitochondria in cancer cells. In: Carney D, Sikora K, editors. Genes and cancer: John Wiley and Sons Ltd; 1990. p. 127–35.
13. Davis S, Weiss MJ, Wong JR, Lampidis TJ, Chen LB. Mitochondrial and plasma membrane potentials cause unusual accumulation and retention of rhodamine 123 by human breast adenocarcinoma-derived MCF-7 cells. J Biol Chem 1985;260:13844–50.
14. Heerdt BG, Houston MA, Anthony GM, Augenlicht LH. Mitochondrial membrane potential (delta psi mt) in the coordination of p53-independent proliferation and apoptosis pathways in human colonic carcinoma cells. Cancer Res 1998;58:2869–75.
15. Heerdt BG, Houston MA, Wilson AJ, Augenlicht LH. The intrinsic mitochondrial membrane potential (Deltapsim) is associated with steady-state mitochondrial activity and the extent to which colonic epithelial cells undergo butyrate-mediated growth arrest and apoptosis. Cancer Res 2003;63:6311–9.
16. Augenlicht LH, Heerdt BG. Mitochondria: integrators in tumorigenesis? Nat Genet 2001;28:104–5.
17. Leibovitz A, Stinson JC, McCombs WB, III, McCoy CE, Mazur KC, Mabry ND. Classification of human colorectal adenocarcinoma cell lines. Cancer Res 1976; 36:4562–9.
18. Heerdt BG, Houston MA, Augenlicht LH. Short-chain fatty acid initiated cell cycle arrest and apoptosis of colonic epithelial cells is linked to mitochondrial function. Cell Growth Differ 1997;8:523–32.
19. Heerdt BG, Houston MA, Mariadason JM, Augenlicht LH. Dissociation of staurosporine induced apoptosis from G2-M arrest in SW620 human colonic carcinoma cells: initiation of the apopotic cascade is associated wtih elevation of the mitochondrial membrane potential (delta psi m). Cancer Res 2000;60:6704–13.
20. Heerdt BG, Houston MA, Anthony GM, Augenlicht LH. Initiation of growth arrest and apoptosis of MCF-7 mammary carcinoma cells by tributyrin, a triglyceride analogue of the short-chain fatty acid butyrate, is associated with mitochondrial activity. Cancer Res 1999;59:1584–91.
21. Mosmann T. Rapid colorimetric assay for cellular growth and survival: application to proliferation and cytotoxicity assays. J Immunol Methods 1983; 65:55–63.
22. Fukazawa H, Nakano S, Mizuno S, Uehara Y. Inhibitors of anchorage-independent growth affect the growth of transformed cell on poly(2-hydroxyethyl methacrylate)-coated surfaces. J Cancer 1996;67:876–82.
23. Salvioli S, Ardizzoni A, Franceschi C, Cossarizza A. JC-1, but not DiOC6(3) or rhodamine 123, is a reliable fluorescent probe to assess changes in intact cells: implications for studies on mitochondrial functionality during apoptosis. FEBS Lett 1997;411:77–82.
24. Reers M, Smith TW, Chen LB. J-aggregate formation of a carbocyanine as a quantitative fluorescent indicator of membrane potential. Biochemistry 1991;30:4480–6.
25. Cossarizza A, Baccarani-Contri M, Kalashnikova G, Franceschi C. A new method for the cytofluorimetric analysis of mitochondrial membrane potential using the J-aggregate forming lipophilic cation 5,5′6,6′-tetrachloro-1,1′3, 3′-tetraethylbenzimidazolcarbocyanine iodide (JC-1). Biochem Biophys Res Commun 1993;30:40–5.
26. Chen Q, Chai YC, Mazumder S, et al. The late increase in intracellular free radical oxygen species during apoptosis is associated with cytochrome *c* release, caspase activation, and mitochondrial dysfunction. Cell Death Differ 2003;10:323–34.
27. Cote C, Poirier J, Boulet D. Expression of the mammalian mitochondrial genome. Stability of mitochondrial translation products as a function of membrane potential. J Biol Chem 1989;264:8487–90.
28. Cote C, Boulet D, Poirier J. Expression of the mammalian mitochondrial genome. Role for membrane potential in the production of mature translation products. J Biol Chem 1990;265:7532–8.
29. Wallace DC. Mitochondrial diseases in man and mouse. Science 1999;283:1482–8.
30. Chandel NS, Maltepe E, Goldwasser E, Mathieu CE, Simon MC, Schumacker PT. Mitochondrial reactive oxygen species trigger hypoxia-induced transcription. Proc Natl Acad Sci U S A 1998;95:11715–20.
31. Wang H-B, Dembo M, Wang Y-L. Substrate flexibility regulates growth and apoptosis of normal but not transformed cells. Am J Physiol 2000;279:C1345–50.
32. Goda N, Dozier SJ, Johnson RS. HIF-1 in cell cycle regulation, apoptosis, and tumor progression. Antioxid Redox Signal 2003;5:467–73.
33. Krishnamachary B, Berg-Dixon S, Kelly B, et al. Regulation of colon carcinoma cell invasion by hypoxia-inducible factor 1. Cancer Res 2003;63:1138–43.
34. Lee MJ, Kim JY, Suk K, Park JH. Identification of the hypoxia-inducible factor 1α-responsive HGTD-P gene as a mediator in the mitochondrial apoptotic pathway. Mol Cell Biol 2004;24:3918–27.
35. Yoon DY, Buchler P, Saarikoski ST, Hines OJ, Reber HA, Hankinson O. Identification of genes differentially induced by hypoxia in pancreatic cancer cells. Biochem Biophys Res Commun 2001;288:882–6.
36. Mathupala SP, Rempel A, Pedersen PL. Glucose catabolism in cancer cells: identification and characterization of a marked activation response of the type II hexokinase gene to hypoxic conditions. J Biol Chem 2001;276:43407–12.
37. Yasuda S, Arii S, Mori A, et al. Hexokinase II and VEGF expression in liver tumors: correlation with hypoxia-inducible factor 1α and its significance. J Hepatol 2004;40:117–23.
38. Schofield CJ, Ratcliffe PJ. Oxygen sensing by HIF hydroxylases. Nat Rev Mol Cell Biol 2004;5:343–54.
39. Goda N, Ryan HE, Khadivi B, McNulty W, Rickert RC, Johnson RS. Hypoxia-inducible factor 1α is essential for cell cycle arrest during hypoxia. Mol Cell Biol 2003;23:359–69.
40. Weinmann M, Marini P, Jendrossek V, et al. Influence of hypoxia on TRAIL-induced apoptosis in tumor cells. Int J Radiat Oncol Biol Phys 2004;58:386–96.
41. Heerdt BG, Houston MA, Augenlicht LH. The intrinsic mitochondrial membrane potential of colonic carcinoma cells is linked to the probability of tumor progression. Cancer Res 2005;65:9861–7.
42. Cayrol C, Knibiehler M, Ducommun B. p21 binding to PCNA causes G1 and G2 cell cycle arrest in p53-deficient cells. Oncogene 1998;16:311–20.
43. Cory S, Adams JM. The Bcl2 family: regulators of the cellular life-or-death switch. Nat Rev Cancer 2002;2:647–56.
44. Marienfeld C, Yamagiwa Y, Ueno Y, et al. Translational regulation of XIAP expression and cell survival during hypoxia in human cholangiocarcinoma. Gastroenterology 2004;127:1787–97.
45. Fossati G, Moulding DA, Spiller DG, Moots RJ, White MR, Edwards SW. The mitochondrial network of human neutrophils: role in chemotaxis, phagocytosis, respiratory burst activation, and commitment to apoptosis. J Immunol 2003;170:1964–72.
46. Diaz G, Setzu MD, Zucca A, et al. Subcellular heterogeneity of mitochondrial membrane potential: relationship with organelle distribution and intercellular contacts in normal, hypoxic and apoptotic cells. J Cell Sci 1999;112:1077–84.
47. Jiang F, Ryan MT, Schlame M, et al. Absence of cardiolipin in the crd1 null mutant results in decreased mitochondrial membrane potential and reduced mitochondrial function. J Biol Chem 2000;275:22387–94.
48. Hardy S, El-Assaad W, Przybytkowski E, Joly E, Prentki M, Langelier Y. Saturated fatty acid-induced apoptosis in MDA-MB-231 breast cancer cells. A role for cardiolipin. J Biol Chem 2003;278:31861–70.
49. Garcia Fernandez M, Troiano L, Moretti L, et al. Changes in intramitochondrial cardiolipin distribution in apoptosis-resistant HCW-2 cells, derived from the human promyelocytic leukemia HL-60. FEBS Lett 2000; 478:290–4.
50. Iigo M, Nakagawa T, Ishikawa C, et al. Inhibitory effects of docosahexaenoic acid on colon carcinoma 26 metastasis to the lung. Br J Cancer 1997;75:650–5.
51. Iwamoto S, Senzaki H, Kiyozuka Y, et al. Effects of fatty acids on liver metastasis of ACL-15 rat colon cancer cells. Nutr Cancer 1998;31:143–50.
52. Vaz FM, Houtkooper RH, Valianpour F, Barth PG, Wanders RJ. Only one splice variant of the human TAZ gene encodes a functional protein with a role in cardiolipin metabolism. J Biol Chem 2003;278:43089–94.
53. Xu Y, Kelley RI, Blanck TJ, Schlame M. Remodeling of cardiolipin by phospholipid transacylation. J Biol Chem 2003;278:51380–5.